J. Membrane Biol. 160, 127–140 (1997)

The Journal of
Membrane
Biology

Subunit Regulation of the Human Brain α_{1E} Calcium Channel

L. Parent[1], T. Schneider[3], C.P. Moore[2], D. Talwar[2]

[1]Département de Physiologie, Membrane Transport Research Group, Université de Montréal, P.O. Box 6128, Downtown Station, Montréal, Qué, H3C 3J7, Canada

[2]Department of Molecular Physiology and Biophysics, Baylor College of Medicine, One Baylor Plaza, Houston, TX 77030, USA

[3]Institute of Neurophysiology, University of Köln, Robert-Koch-str 39, D-50931, Köln, Germany

Received: 27 March 1997/Revised: 10 July 1997

Abstract. The α_1 subunit coding for the human brain type E calcium channel (Schneider et al., 1994) was expressed in *Xenopus* oocytes in the absence, and in combination with auxiliary $\alpha_2\delta$ and β subunits. α_{1E} channels directed with the expression of Ba^{2+} whole-cell currents that completely inactivated after a 2-sec membrane pulse. Coexpression of α_{1E} with $\alpha_{2b}\delta$ shifted the peak current by +10 mV but had no significant effect on whole-cell current inactivation. Coexpression of α_{1E} with β_{2a} shifted the peak current relationship by −10 mV, and strongly reduced Ba^{2+} current inactivation. This slower rate of inactivation explains that a sizable fraction ($40 \pm 10\%$, $n = 8$) of the Ba^{2+} current failed to inactivate completely after a 5-sec prepulse. Coinjection with both the cardiac/brain β_{2a} and the neuronal $\alpha_{2b}\delta$ subunits increased by ≈10-fold whole-cell Ba^{2+} currents although coinjection with either β_{2a} or $\alpha_{2b}\delta$ alone failed to significantly increase α_{1E} peak currents. Coexpression with β_{2a} and $\alpha_{2b}\delta$ yielded Ba^{2+} currents with inactivation kinetics similar to the β_{2a} induced currents, indicating that the neuronal $\alpha_{2b}\delta$ subunit has little effect on α_{1E} inactivation kinetics. The subunit specificity of the changes in current properties were analyzed for all four β subunit genes. The slower inactivation was unique to α_{1E}/β_{2a} currents. Coexpression with β_{1a}, β_{1b}, β_3, and β_4, yielded faster-inactivating Ba^{2+} currents than currents recorded from the α_{1E} subunit alone. Furthermore, $\alpha_{1E}/\alpha_{2b}\delta/\beta_{1a}$; $\alpha_{1E}/\alpha_{2b}\delta/\beta_{1b}$; $\alpha_{1E}/\alpha_{2b}\delta/\beta_3$; $\alpha_{1E}/\alpha_{2b}\delta/\beta_4$ channels elicited whole-cell currents with steady-state inactivation curves shifted in the hyperpolarized direction. The β subunit-induced changes in the properties of α_{1E} channel were comparable to modulation effects reported for α_{1C} and α_{1A} channels with $\beta_3 \approx \beta_{1b} > \beta_{1a} \approx \beta_4 \gg \beta_{2a}$ inducing fastest to slowest rate of whole-cell inactivation.

Key words: *Xenopus* oocytes — Calcium channel — β subunit — $\alpha_2\delta$ subunit — Inactivation — Neuronal cells

Introduction

Voltage-dependent Ca^{2+} channels are multiprotein complexes composed of at least three subunits: α_1; $\alpha_2\delta$; and β subunits (Catterall, 1991). The biochemistry of skeletal muscle Ca^{2+} channels has provided strong evidence that the α_1 subunit forms a complex with three auxiliary subunits ($\alpha_2\delta$, β_1, γ). Although a minimum voltage-gated Ca^{2+} channel can be formed by a single α_1 subunit, coexpression of the full complement of subunits is required for the cardiac L-type α_{1C} (Singer et al., 1991); brain N-type α_{1B} (Williams et al., 1992*b;* Stea et al., 1993); brain L-type α_{1D} (Williams et al., 1992*a*); brain P/Q type α_{1A} (Sather et al., 1993; DeWaard & Campbell, 1995) to generate Ca^{2+} and Ba^{2+} currents with time course and voltage-dependence similar to the native Ca^{2+} currents. Recombinant calcium channel kinetics were shown to be sensitive to interacting subunits. Both activation and inactivation kinetics appear to be affected by auxiliary β and $\alpha_2\delta$ subunits in a way that is strongly dependent upon the molecular identity of the interacting subunits.

Molecular cloning has shown that β subunits are encoded by four nonallelic genes; skeletal β_1, heart/brain β_2, brain β_3, brain β_4 (Ruth et al., 1989; Hullin et al., 1992; Perez-Reyes et al., 1992; Castellano et al., 1993*a*,*b*). Cross-hybridization of β subunit cDNA showed that the β_2 subunit (β_{2a} and β_{2b} splice variants) and the β_3 subunit are both expressed in brain (Hullin et

Correspondence to: L. Parent

al., 1992; Perez-Reyes et al., 1992; Castellano et al., 1993*a*). Most expressed combinations of α_1 and β subunits known to date result in current amplitude stimulation (Perez-Reyes et al., 1992; Hullin et al., 1992; Mori et al., 1991; Williams et al., 1992*a;* Ellinor et al., 1993; Sather et al., 1993) and/or modifications of whole-cell current kinetics (Lacerda et al., 1991; Varadi et al., 1991; Lory et al., 1993; Castellano et al., 1993*a,b*). The different β subunits have quantitatively distinct effects, indicating that channel assembly has important functional effects on calcium channel activity. The pattern of influence of various β subunits on the rate of inactivation were shown to be similar for the brain α_{1A} (Sather et al., 1993; DeWaard & Campbell, 1995); and the cardiac α_{1C} (Hullin et al., 1992) with $\beta_3 > \beta_1 > \beta_2$ subunits with β_3 producing the fastest rate of inactivation.

The α_2 and δ subunits are encoded by the same gene and their disulfide bonds are proteolytically cleaved in post-translational reactions. Only one $\alpha_2\delta$ calcium channel subunit gene has been identified but five $\alpha_2\delta$ splice variants have been reported in different tissues (Ellis et al., 1988; Brust et al., 1993) with the $\alpha_{2b}\delta$ transcript being predominantly expressed in the central nervous system (Williams et al., 1992*a*). The rabbit skeletal $\alpha_{2b}\delta$ (Ellis et al., 1988) and human neuronal $\alpha_{2b}\delta$ (Williams et al., 1992*a*) subunits are 97% identical at the primary structure level. The most recent topological model shows the $\alpha_2\delta$ subunit as a mostly extracellular protein with a single transmembrane segment corresponding to the sequence of the δ subunit (Brickley et al., 1995; Gurnett, DeWaard & Campbell, 1996). Functional expression of the $\alpha_2\delta$ subunit results in 2- to 10-fold stimulation of α_{1C}; α_{1A}; α_{1D} current amplitude (Mori et al., 1991; Hullin et al., 1992; Williams et al., 1992*a;* Brust et al., 1993; DeWaard & Campbell, 1995).

Because any of the α_1 and β subunit combination is possible in vivo calcium channels, numerous kinetic variations can be produced by small differences in subunit interactions. Combinatorial analysis suggests that 20 different neuronal calcium channels can be produced by the combination of the five α_1 and four β subunit genes found in brain tissues. This number of possible channel kinetic behavior could be further augmented by any significant contribution from the neuronal $\alpha_{2b}\delta$ subunit. We thus undertook a thorough investigation of the interaction of the α_{1E} subunit with auxiliary $\alpha_{2b}\delta$ and β subunits specifically identified in brain. Part of these results were presented earlier in an abstract form (Rodriguez, Schneider & Parent, 1996).

Materials and Methods

Recombinant DNA Techniques

Standard methods of plasmid DNA preparation are being used (Sambrook, Fritsch & Manitas, 1989). The human brain α_{1E} subunit (Schneider et al., 1994) is 96% homologous to the rabbit BII-1 clone (Niidome et al., 1992) and 94% homologous to the rat α_{1E} clone (Soong et al., 1993). The deduced molecular weight of the proteins are 242 kD ($\alpha_{1C\text{-}a}$); 262 kD (α_{1E}); 68 kD (β_{2a}); 123 kD ($\alpha_{2b}\delta$). The wild-type cardiac $\alpha_{1C\text{-}a}$ subunit cDNA (Genbank accession number X15539) was cloned from rabbit (Perez-Reyes et al., 1990; Wei et al., 1991). A double-deleted version of α_{1C}, the α_{1C} ΔNΔC, that has been previously shown to generate 3 to 5-fold larger currents than the full-length α_{1C} (Wei et al., 1994*a,b*) was used in this study. The DNA constructs α_{1E} and α_{1C} were linearized at the 3′ end by *Hind III* digestion. The rat brain $\alpha_{2b}\delta$ subunit was linearized by *EcoR I* digestion and the rat brain $\beta_{1..4}$ subunits by *Not I* digestion. Runoff transcripts were prepared using methylated cap analogue $m^7G(5')ppp(5')G$ and T7 RNA polymerase with the mMessagemMachine® transcription kit (Ambion, Austin, TX). The cRNA product was resuspended in 0.1 M KCl and stored at −80°C. The integrity of the final product and the absence of degraded RNA was determined by a denaturing agarose gel stained with ethidium bromide.

Functional Expression of Recombinant Calcium Channels

Female *Xenopus laevis* clawed frog (Nasco, Fort Atkinson, WI) were anesthetized by immersion in 0.1% tricaine or MS-222 (3-aminobenzoic acid ethyl ester, Sigma) for 15–30 min before surgery (Parent et al., 1995*a,b*). Ovarian tissue was removed via a small incision in the abdomen and individual oocytes (stage V or VI) free of follicular cells are obtained after 30–40 min incubation in a calcium-free solution OR-2 (in mM: 82.5 NaCl; 2.5 KCl; 1 $MgCl_2$; 5 Hepes; pH 7.6) containing 2 mg/ml collagenase (Gibco, Grand Island, NY). Carefully selected stage V and VI oocytes were injected 16 hr later with 47 nl of cRNA coding for the given α_1 subunit at a concentration of 100 ng/ml (4.7 ng cRNA). When stated, the α_1 subunit was co-injected with the following auxiliary subunits: the rat brain $\alpha_{2b}\delta$ (gift from Dr. Terry P. Snutch, UBC, Vancouver, Canada) and skeletal β_{1a} (Ruth et al., 1989) and brain β_{1b}; cardiac β_{2a} (Perez-Reyes et al., 1992); brain β_3 (Castellano et al., 1993*a*); brain β_4 (Castellano et al., 1993*b*) in a 1:1:2 molar ratio ($\alpha_1/\alpha_2\delta/\beta$). Oocytes were incubated at 19°C under gentle shaking for 3 to 7 days in a SOS solution (in mM): 100 NaCl; 2 KCl; 1.8 $CaCl_2$; 1 $MgCl_2$; 5 HEPES; 2.5 pyruvic acid; 100 units/ml of penicillin; 50 mg/ml gentamicin; pH 7.6. Solutions were changed daily.

Electrophysiological Recordings

Whole-cell currents were recorded at room temperature with a two-electrode voltage-clamp amplifier (OC-725B, Warner Instruments). Voltage and current electrodes (0.5–2 MΩ tip resistance) were filled with 3 M KCl; 1 mM EGTA; 10 mM HEPES (pH 7.4) and bath electrodes were filled with the same solution in 3% agar. Oocytes were first impaled in a modified Ringer solution (in mM): 96 NaOH; 2 KOH; 1.8 $CaCl_2$; 1 $MgCl_2$; 10 HEPES titrated to pH 7.4 with methane sulfonic acid (MeS), then the bath solution was exchanged with the appropriate test solution. Whole-cell currents were typically measured with a 10 Ba^{2+} solution (in mM; 10 $Ba(OH)_2$; 110 NaOH; 1 KOH; 0.5 niflumic acid; 10 Hepes titrated to pH 7.2 with methane sulfonic acid CH_3SO_3H); in a 10 CaMeS solution where $Ca(OH)_2$ replaced $Ba(OH)_2$ equimolarly; and in a 120 LiMeS solution (in mM: 120 LiOH; 5 EGTA, 2 KOH; 10 Hepes titrated to pH 7.3 with methane sulfonic acid). Rare frog batches where endogenous channels generate Ba^{2+} currents higher than 50 nA were systematically discarded. To minimize kinetic contamination by the endogenous Ca^{2+} activated Cl^- current, oocytes were

directly injected with 50 nl of a Bapta (1,2-bis(2-aminophenoxy)ethane N,N,N′, N-tetraacetic acid) (Sigma, St-Louis, MO) solution (10 mM Bapta, 10 mM Hepes, pH 7.4) 1 hr prior to experiments. In some experiments, oocytes were preincubated in the presence of 100 μM Bapta-AM (Calbiochem, San Diego, CA), a membrane-permeable analogue of Bapta, for two hours prior to experiments with similar results. Oocytes were superfused by gravity flow at a rate of 5 ml/min. Voltage pulses were applied from a holding potential of −80 mV at a frequency of 0.2 Hz. Capacitive transients and leak currents were subtracted from the whole-cell current traces using the residual currents measured in the presence of 1 mM $CoCl_2$. PClamp software Clampex 6.02 (Axon instruments, Foster City, CA) was used for online data acquisition. Unless stated otherwise, data were sampled at 10 kHz and filtered at 2 kHz.

Data Analysis

Steady-state inactivation h_∞ were measured using a multistep protocol at the end of a 5-sec prepulse (Parent et al., 1995).

$$\frac{i}{i_{\max}} = 1 - \frac{RT}{F}\frac{1 - Y_o}{1 + \{\exp - z(V_m - E_{0.5})\}} \quad (1)$$

For each series of experiments, data points were normalzed to the peak current (i/i_{max}) and were plotted against the prepulse voltage. Steady-state inactivation data points were obtained from pooled data (mean ± SEM, $n \leq 3$) and were fitted to the modified Boltzmann Eq. 1 with $E_{0.5}$, midpoint potential; z, slope parameter; Y_o, fraction of noninactivating current; V_m, the prepulse potential, and RT/F with their usual meanings.

For the activation and inactivation time constants, leak subtracted current traces recorded at 10 kHz were fitted to bi- or tri-exponential functions (Eq. 2) at $t = 300$ msec using Clampfit (PClamp 6.02, Axon Instruments, Foster City, CA).

$$I(t) = I_{act}\exp\left(-\frac{t-k}{\tau_{act}}\right) + I^1{}_{inact}\exp\left(-\frac{t-k}{\tau^1{}_{inact}}\right) + I^2{}_{inact}\exp\left(-\frac{t-k}{\tau^2{}_{inact}}\right) + C \quad (2)$$

where $I(t)$ is the current at time t; τ_{act}; $\tau^1{}_{inact}$; $\tau^2{}_{inact}$ are the time constants of the activation and inactivation processes; I_{act}; $I^1{}_{inact}$; $I^2{}_{inact}$ are the amplitude of these processes; and k and C are fitting constants. For whole-cell peak current expression (Table 1), data were all collected in the same oocyte batch since mRNA translational efficiency was found to somewhat vary from batch to batch. The Ca^{2+} affinity of α_{1E} channels was measured as previously described (Parent & Gopalakrishnan, 1995). Whole-cell currents were measured in a 120 mM Li^+ solution (*see above*) where the free Ca^{2+} concentration adjusted with EGTA and $CaCl_2 2H_2O$ according to Fabiato and Fabiato (1979). Normalized peak currents were plotted against the log of the free Ca^{2+} concentration and fitted to single inhibition equations (Parent & Gopalakrishnan, 1995).

Results

Expression of Functional α_{1E} Calcium Channels

Expression of neuronal calcium channel α_{1A} and α_{1B} subunits alone generally results in low current density (Mori et al., 1991; Stea et al., 1993; Sather et al., 1993; DeWaard & Campbell, 1995). In many cases, the current densities are so low that accurate biophysical characterization cannot be performed unless auxiliary β subunits are co-expressed. The human brain α_{1E} calcium channel expresses μA of inward Ba^{2+} currents when expressed alone in *Xenopus* oocytes. This property makes the human brain α_{1E} a suitable candidate to study subunit interactions in neuronal calcium channels. Macroscopic currents recorded from oocytes expressing of α_{1E} subunits are shown in Fig. 1. Contrary to recombinant α_{1C} channels, every α_{1E} channel combination tested, generated stable whole-cell currents with <10% rundown over a 20-min period. In Fig. 1, whole-cell currents were recorded in the presence of 120 mM Li^+ (top left), 10 mM Ba^{2+} (top right), and 10 mM Ca^{2+} (bottom left). As compared to whole-cell currents recorded from recombinant α_{1C} channels (Parent et al., 1995), α_{1E} channels inactivated in the presence of Li^+ and in the absence of auxiliary subunits. Since the biophysical separation between voltage- and calcium-dependent inactivation has been classically achieved by characterizing the rate of current inactivation in the presence of Ba^{2+} *vs.* Ca^{2+}, inactivation of α_{1E} can be said to be mostly dependent upon the membrane potential. However, the rate of inactivation

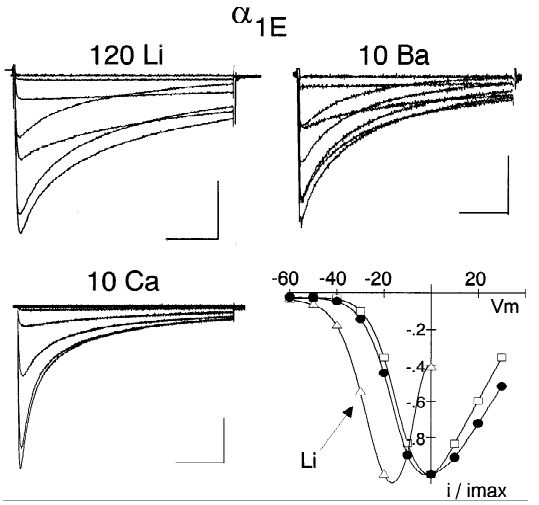

Fig. 1. The whole-cell current α_{1E} kinetics are relatively insensitive to the nature of the charge carrier. The current traces were measured after injection of the α_{1E} subunit alone in the presence of (10 mM): 120 Li^+ (upper left); 10 Ba^{2+} (upper right); and 10 Ca^{2+} (lower left) after injection of 10 Bapta. Holding potential was −80 mV throughout. 450 msec voltage pulses were applied from −60 to +30 mV. Inactivation time constants were $\tau_{inact} = 217$ msec (120 mM Li^+); $\tau^1{}_{inact} = 20$ and $\tau^2{}_{inact} = 158$ msec (10 mM Ba^{2+}); $\tau^1{}_{inact} = 21$ and $\tau^2{}_{inact} = 137$ msec (10 mM Ca^{2+}) at $V_m = -10$ mV. Capacitive transients were erased for the first ms after the voltage step. Corresponding normalized peak *I-V* relationships are shown at the lower right. Current traces recorded in the presence of Li^+ (◁) activated around −50 mV and peaked at −20 mV. Current traces recorded in the presence of 10 mM Ba^{2+} (□) and 10 mM Ca^{2+} (●) activated around −40 mV and peaked at 0 mV. Current and time scales are 1 μA and 100 msec throughout.

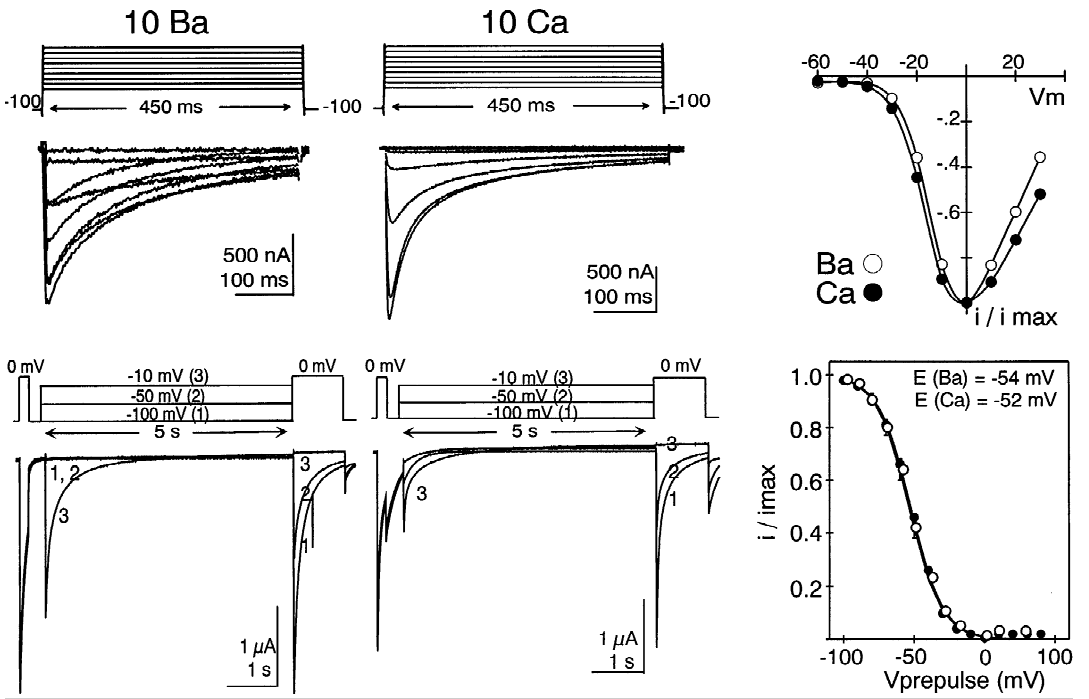

Fig. 2. *Upper Panel.* Macroscopic current-voltage relationships were recorded in the presence of 10 mM Ba^{2+} (left) and 10 mM Ca^{2+} (middle) after Bapta injection. 450-msec-voltage pulses were applied from a holding potential of −100 mV. Ba^{2+} and Ca^{2+} current traces showed similar rates of inactivation. Furthermore, Ba^{2+} ($n = 4$) and Ca^{2+} ($n = 5$) displayed similar whole-cell conductances as shown on the peak current-voltage relationship (right). Error bars are SEM. *Lower Panel.* Steady-state inactivation curves for α_{1E} are identical for Ba^{2+} and Ca^{2+} ions. Inactivation was measured after a series of 14 prepulse (5 sec each) were applied in the presence of 10 mM Ba^{2+} (left) and 10 mM Ca^{2+} (middle) after Bapta injection. *Vh* = −100 mV throughout. The relative mean normalized current was fitted to Eq. 1, a Boltzmann-like function described in Materials and Methods (right). Each curve was obtained from the mean of 4 independent recordings. Error bars are SEM. Whole-cell currents inactivated completely with a midpoint of inactivation $E_{0.5} = -54$ mV (Ba^{2+}) and −52 mV (Ca^{2+}). Fits were indistinguishable with identical slope factors $z = 2.2$.

was somewhat slower in the complete absence of divalent cations with $Li^+ < Ba^{2+} < Ca^{2+}$. As seen, the Li^+ current (120 mM Li^+, 5 mM EGTA) peaked shortly after the voltage step with $\tau_{act} = 2 \pm 1$ msec ($n = 3$) and inactivated during the 450 msec-pulse at $V_m = -10$ mV with 2 time constants $\tau^1_{inact} = 18 \pm 2$ msec ($n = 3$) and $\tau^2_{inact} = 257 \pm 34$ msec ($n = 3$). In contrast, divalent whole-cell currents were described by $\tau_{act} = 2 \pm 0.5$ msec ($n = 7$) and $\tau^1_{inact} = 18 \pm 3$ msec ($n = 3$) and $\tau^2_{inact} = 138 \pm 27$ msec ($n = 3$) for 10 mM Ca^{2+} and $\tau^1_{inact} = 18 \pm 4$ ms ($n = 4$) and $\tau^2_{inact} = 158 \pm 18$ msec ($n = 4$) for 10 mM Ba^{2+}, which are not significantly different. Our data contrast with the results reported for the human $\alpha_{1E\text{-}3}$ expressed in HEK-293 cells, that displayed slower inactivation in the presence of Ca^{2+} (Williams et al., 1994). Similar results, showing slightly faster Ca^{2+} current traces, were also obtained for other channel combinations such as α_{1E}/α_{1E}, $\alpha_{1E}/\alpha_{2b}\delta/\beta_{1a}$ α_{1E}/β_3 and α_{1E}/β_{2a} calcium channels (*results not shown*). There is thus a small but notable contribution of the charge carrier to the inactivation kinetics of α_{1E} channels. Recombinant human α_{1E} channels remained nonetheless faster ($\tau_{inact} < 300$ msec) than recombinant α_{1C} channels whether the current was carried by monovalent or divalent cations. In addition, the normalized peak current relationship (Fig. 1, bottom right) shows that the Ba^{2+} (□) and the Ca^{2+} (●) current-voltage relationships were similar with activation threshold of −40 mV and peak currents at 0 mV. As expected for monovalent cations, the Li^+ current-voltage relationship was shifted in the hyperpolarized direction, with an activation threshold around −50 mV and a peak current at −20 mV.

It is unlikely that the slight increased inactivation shown in Fig. 1 was caused by a corresponding increase in macroscopic conductance since whole-cell Li^+, Ba^{2+}, and Ca^{2+} peak currents were not significantly different. In contrast to recombinant cardiac α_{1C} channels (Parent et al., 1995), Fig. 2 (top) shows that α_{1E} carried Ba^{2+} and Ca^{2+} ions with the same whole-cell conductance. The voltage-dependence of inactivation was not significantly affected by the nature of the divalent cation between Ba^{2+} and Ca^{2+} (*see* Fig. 2, bottom panel). Steady-state inactivation was reported for α_{1E} channels in the presence of 10 mM Ba^{2+} or in the presence of 10 mM Ca^{2+}, by measuring the relative current obtained at the end of a 5-sec prepulse. Fraction of the inactivating current (*i*/imax or *i* relative) was obtained from the ratio of the peak current measured at the test potential of 0 mV before and

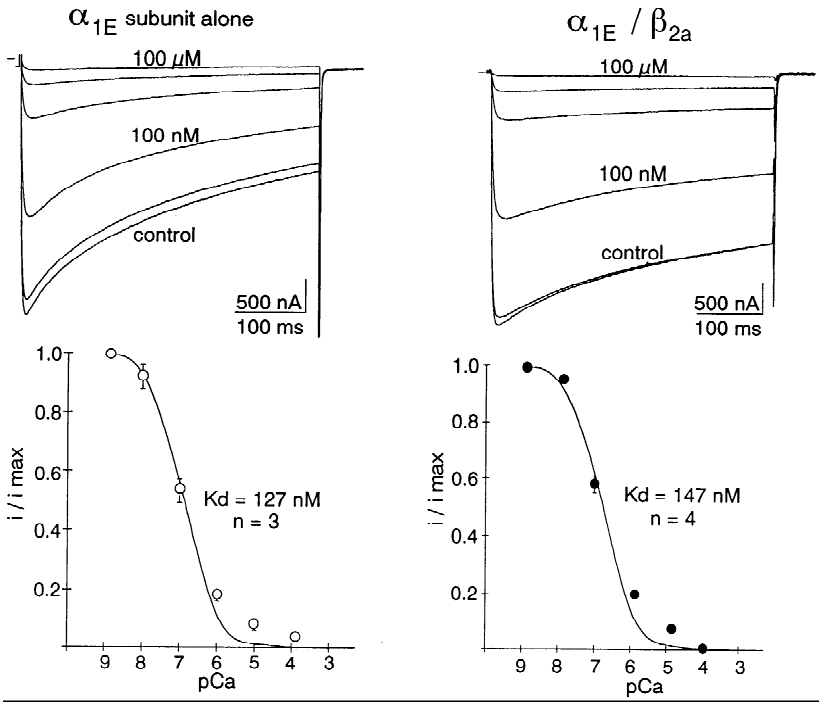

Fig. 3. Calcium block of whole-cell Li^+ currents for α_{1E} (left) and α_{1E}/β_{2a} provided additional evidence that Ca^{2+} affinity requires glutamate residues in the SS2 region of the P-loop. Ca^{2+} block was estimated from the decrease in the whole-cell peak current, as measured in the presence of 120 mM Li^+ + 5 mM EGTA at $V_m = -20$ mV, after perfusion with a Ca^{2+} solution. Normalized currents were plotted against the −log[free Ca^{2+}] and fitted to single inhibition curves. Data were found to deviate from the one-site model at higher Ca^{2+} which could be explained by the multi-ion nature of the calcium channel pore. Coexpression with β_{2a} subunit did not alter channel affinity for Ca^{2+} although whole-cell currents appeared significantly slower. Kd = 0.13 ± 0.02 μM for α_{1E} ($n = 3$) and Kd = 0.14 ± 0.02 μM ($n = 4$) for α_{1E}/β_{2a} channels.

after the 5-sec prepulse. Each set of experiments was performed in triplicate after preincubation with 100 μM Bapta-AM or after injection of 10 mM Bapta-Hepes (final $[Bapta]_i \approx 10$ μM). The mean fractional current was then fitted to a modified Boltzmann equation (Eq. 1) where $E_{0.5}$ is the mid-inactivation potential. Ba^{2+} and Ca^{2+} macroscopic currents inactivated completely at the end of a 5-sec prepulse with $E_{0.5} = -54$ mV for Ba^{2+} and $E_{0.5} = -52$ mV for Ca^{2+}. Fits were indistinguishable with identical z parameters = 2.2 for inactivation measured with 10 mM Ba^{2+} and 10 mM Ca^{2+}.

The pore region of the α_{1E} calcium channel gene displays high primary sequence homology to other α_1 calcium channel genes such as α_{1C}. Among other similarities, α_{1E} possesses the ring of four glutamate residues known to play a major role in Ca^{2+}/Na^+ selectivity in calcium channels (Yang et al., 1993; Parent & Gopalakrishnan, 1995). The presence of the glutamate ring in pores I, II, III, IV predicts that α_{1E} should also display high affinity for Ca^{2+}. Experiments performed with α_{1E} and α_{1E}/β_{2a} channels confirmed that the brain α_{1E} channel has a high affinity, in the μM range, for Ca^{2+}. As we had previously demonstrated for recombinant α_{1C} channels, whole-cell Li^+ current can be progressively blocked by increasingly larger Ca^{2+} concentrations added to the bath. Figure 3 shows the actual current traces. Whole-cell Li^+ currents were large, usually around 4 μA, in the complete absence of added Ca^{2+} and in the presence of 5 mM EGTA. The addition of Ca^{2+} to the bath progressively reduced this current with 100 μM Ca^{2+} blocking all whole-cell currents. Ca^{2+} block measured under these conditions was easily reversible after washout with EGTA in the bath. The relative current plotted as a function of the free Ca^{2+} concentration was fitted by a single inhibition curve with a Kd of 0.127 μM for α_{1E} and 0.147 μM for α_{1E}/β_{2a}, values which are not significantly different from what we reported for Ca^{2+} affinity for the wild-type α_{1C} (Parent & Gopalakrishnan, 1995). Ca^{2+} affinity was not influenced by the coexpression with the β_{2a} subunit, however the whole-cell current traces were significantly slower in the presence of the β_{2a} subunit. For instance, 60% of the Li^+ whole-cell α_{1E} currents had decayed after a 400-msec pulse to −20 mV as compared to only 30% of the whole-cell current for α_{1E}/β_{2a} channels. This significant difference in whole-cell current inactivation kinetics prompted us to study in detail auxiliary subunit regulation of α_{1E} currents.

Recombinant α_{1E} Calcium Channels are Modulated by $\alpha_{2b}\delta$ and β_{2a} Subunits

Previous studies have shown that β subunits are important regulators of the α_1 subunit activation and inactivation kinetics, such that β are said to ''normalize'' recombinant cardiac Ca^{2+} channel kinetics (Lacerda et al., 1991; Singer et al., 1991; Hullin et al., 1992) and pharmacology (Wei et al., 1995). While the effects of β subunits on α_{1E} channels have been well documented (Schneider et al., 1994; Olcese et al., 1994), $\alpha_2\delta$ subunit regulation of α_{1E} calcium channels remains unclear (Wakamori et al., 1994). To achieve a comprehensive

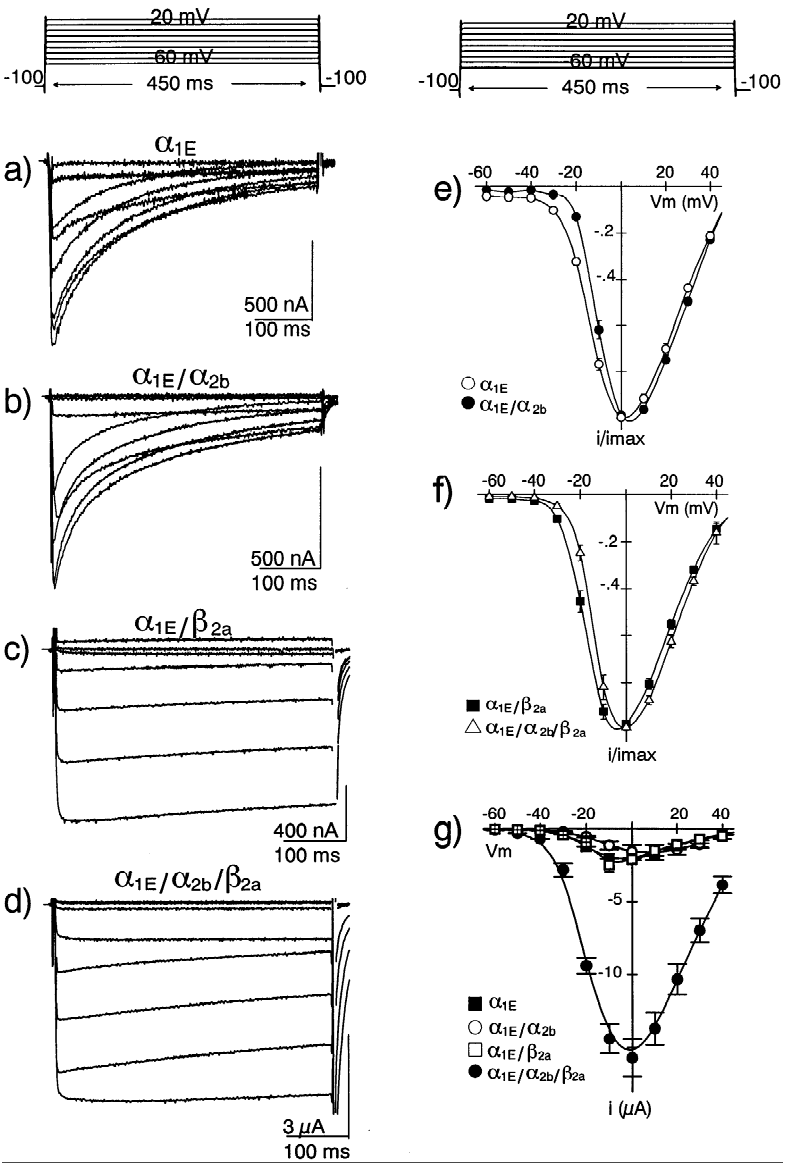

Fig. 4. Modulation of α_{1E} channels by $\alpha_{2b}\delta$ and β_{2a} channels. *Left panel.* Whole-cell current traces for recombinant α_{1E} channels were recorded in the presence of 10 mM Ba^{2+}. From top to bottom, are shown; (*A*) α_{1E} alone; (*B*) $\alpha_{1E}/\alpha_{2b}\delta$; (*C*) α_{1E}/β_{2a}; and (*D*) $\alpha_{1E}/\alpha_{2b}\delta/\beta_{2a}$. Triplicate experiments were carried out on the same day. Holding potential was −100 mV. Approximately 70% of the α_{1E} currents inactivated during a 450 msec pulse at +10 mV. In contrast, only 22% of the current inactivated when α_{1E} was coexpressed in a 1:1 ratio with β_{2a}. As seen, $\alpha_{1E}/\alpha_{2b}\delta/\beta_{2a}$ kinetics are not significantly different from α_{1E}/β_{2a} current kinetics. At +20 mV, whole-cell current activated with $\tau_{act} = 1$ msec (α_{1E} and $\alpha_{1E}/\alpha_{2b}\delta$) and $\tau_{act} = 4$ msec ($\alpha_{1E}/\alpha_{2b}\delta/\beta_{2a}$). Inactivation time constants were $\tau_{inact} = 98$ msec (α_{1E}); $\tau_{inact} = 87$ msec ($\alpha_{1E}/\alpha_{2b}\delta$); $\tau_{inact} = 202$ msec ($\alpha_{1E}/\alpha_{2b}\delta/\beta_{2a}$). Coexpression with either β_{2a} or $\alpha_{2b}\delta$ failed to increase the macroscopic barium α_{1E} current but coexpression with both β_{2a} and $\alpha_{2b}\delta$ resulted in a 10-fold increase in the whole-cell current suggesting a synergistic effect of auxiliary subunits on the α_{1E} subunit. *Right panel.* (*E*) Normalized peak current-voltage relationships (*I-V*) are reported for α_{1E} (○) and $\alpha_{1E}/\alpha_{2b}\delta$ (●). The mean of 3–5 experiments, for each channel composition, is shown with the SEM. Error bars appear smaller than the data point. The neuronal $\alpha_{2b}\delta$ subunit showed no discernible effect on the rate of α_{1E} inactivation but significantly shifted the peak current from 0 to +10 mV. (*F*) Normalized peak current-voltage relationships (*I-V*) are reported to α_{1E}/β_{2a} (■) and $\alpha_{1E}/\alpha_{2b}\delta/\beta_{2a}$ (▽). Further coinjection with the neuronal $\alpha_{2b}\delta$ subunit does not significantly modify the rate of inactivation of α_{1E}/β_{2a} but shifted the macroscopic current-voltage relationship back to the right from −10 mV (α_{1E}/β_{2a}) to 0 mV ($\alpha_{1E}/\alpha_{2b}\delta/\beta_{2a}$). (*G*) Expression of the human α_{1E} subunit with β_{2a} and $\alpha_{2b}\delta$ subunits increased ≈10-fold expression levels, dramatically slowed current inactivation, and reset the whole-cell peak current to 0 mV. On this figure as well as on the following ones, α_2 and α_{2b} stand systematically for $\alpha_{2b}\delta$. Time scales are 100 msec throughout.

understanding of the mechanisms controlling brain α_{1E} channel properties, we have coexpressed the α_{1E} subunit with and without β_{1a}, β_{1b}, β_{2a}, β_3, β_4, and $\alpha_{2b}\delta$ subunits. Figure 4 shows whole-cell current traces obtained with the human brain α_{1E} subunit (*A*) coinjected with either $\alpha_{2b}\delta$ (*B*); β_{2a} (*C*); or both $\alpha_{2b}\delta/\beta_{2a}$ (*D*) subunits in the presence of 10 mM Ba^{2+}. Corresponding peak *I-V* curves are shown to the right (*E,F,G*). From these experiments, coexpression with neuronal $\alpha_{2b}\delta$ subunit appeared to show little influence on α_{1E} channel inactivation kinetics. At −10 mV, the macroscopic currents were described by similar time constants with $\tau_{act} = 2 \pm 0.6$ msec; $\tau^1_{inact} = 21 \pm 5$ msec and $\tau^2_{inact} = 149 \pm 20$ msec ($n = 5$) for α_{1E} channels as compared to $\tau_{act} = 2 \pm 1$ msec; $\tau^1_{inact} = 22 \pm 3$ msec and $\tau^2_{inact} = 169 \pm 23$ msec ($n = 3$) for $\alpha_{1E}/\alpha_{2b}\delta$ channels. However, coexpressing

Table 1. α_{1E} peak current expression as a function of $\alpha_{2b}\delta$ and β_{2a}

Subunit composition	Mean peak current ± SEM	*n*	Batch
α_{1E}	−1.3 ± 0.4 μA	10	X814
$\alpha_{1E}/\alpha_{2b}\delta$	−1.6 ± 0.6 μA	4	X814
α_{1E}/β_{2a}	−1.7 ± 0.5 μA	6	X814
$\alpha_{1E}/\alpha_{2b}\delta/\beta_{2a}$	−15.3 ± 5.2 μA	6	X814

Comparison of the peak current amplitudes obtained for various α_{1E} channel compositions. Since mRNA translational efficiency was found to vary between batches, all data reported here were collected within the same oocyte batch. The number *n* of experiments for each channel is indicated. Data are mean ± SEM. Currents were measured with 10 mM Ba^{2+} as the charge carrier. Holding potential was −80 mV.

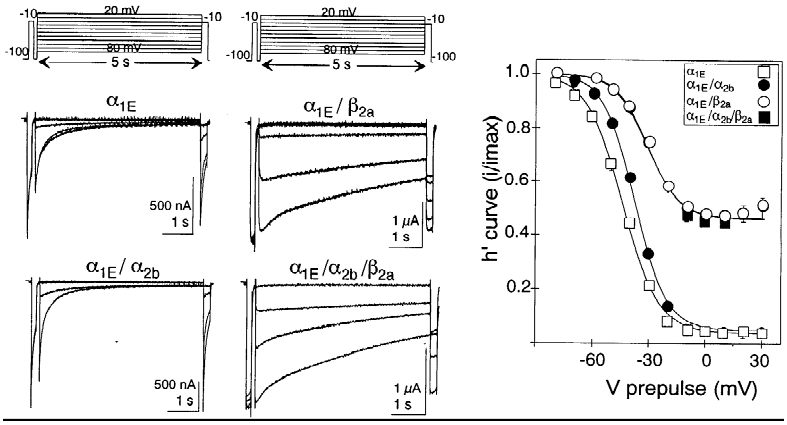

Fig. 5 *Left panel.* Steady-state inactivation of recombinant α_{1E} calcium channels. Whole-cell currents were measured in the presence of 10 mM Ba^{2+}. Steady-state inactivation was measured at 0 mV after a 5-sec prepulse applied from −100 to +20 mV. Current inactivation was measured at the test potential of 0 mV. Holding potential was −100 mV and pulses were applied at a frequency of 0.1 Hz. Data were filtered at 1 kHz. Triplicate experiments were performed the same day for each experimental condition. *Right panel.* Inactivation was reported as the fractional peak current as a function of the prepulse voltage. Mean data of 3 to 5 independent experiments was fitted to a Boltzmann-like function (Eq. 1). Under these conditions, whole-cell current inactivated completely for α_{1E} with $E_{0.5} = -44$ mV and for $\alpha_{1E}/\alpha_{2b}\delta$ with $E_{0.5} = -38$ mV. However, a significant fraction (44%) of the whole-cell current generated by α_{1E}/β_{2a} and $\alpha_{1E}/\alpha_{2b}\delta/\beta_{2a}$ remained after the 5-sec prepulse with $E_{0.5} = -31$ mV. Estimated slope factors from the fit were $z = 2.3$ for α_{1E}; $z = 2.5$ for $\alpha_{1E}/\alpha_{2b}\delta$; $z = 2.4$ for α_{1E}/β_{2a} and for $\alpha_{1E}/Ba^{2+}/\alpha_{2b}\delta$.

α_{1E} channels with $\alpha_{2b}\delta$ clearly shifted the peak *I-V* curve toward more depolarized potentials (*E*). Macroscopic currents peaked at 10 ± 2 mV ($n = 10$) for $\alpha_{1E}/\alpha_{2b}\delta$ channels as compared to 0 ± 3 mV ($n = 10$) for α_{1E} channels. This result contrasts with the complete absence of regulation by the same $\alpha_{2b}\delta$ subunit on α_{1A} channels when injected in the absence of a β subunit (DeWaard & Campbell, 1995). In this latter paper it was shown that $\alpha_{2b}\delta$ failed to modify the peak *I-V* curve, activation and inactivation kinetics of α_{1A} channels.

Coinjection with the auxiliary subunit β_{2a} from rat brain (Perez-Reyes et al., 1992) slowed down the rate of inactivation of α_{1E} channels. As seen earlier, the time course of inactivation of the α_{1E} subunit recorded in the presence of 10 mM Ba^{2+} can be described by a sum of 2 exponential functions ($\tau^1_{inact} = 18$ msec; $\tau^2_{inact} = 148$ msec) at −10 mV. Coinjection with β_{2a} appeared to have eliminated the fast component of inactivation τ^1_{inact} and further decreased the slow component τ^2_{inact} to 655 ± 43 msec ($n = 6$). Furthermore, the relative contribution of τ_{inact} to τ_{act} decreased from 56 ± 8% ($n = 4$) for α_{1E} alone to 19 ± 9% ($n = 6$) in α_{1E}/β_{2a} whole-cell current recordings. This decrease in the rate of inactivation after coexpression with β_{2a} was observed at all membrane potentials between −20 to +30 mV. Noteworthy, the slowing of α_{1E} kinetics was also observed in the presence of 120 mM Li^+ and 10 mM Ca^{2+} as charge carriers (*results not shown*). This observation has important physiological implications since both α_{1E} and β_{2a} could be expressed together in neurons. Coinjection with β_{2a} alone shifted the α_{1E} peak current by −10 mV along the voltage axis (from +10 to 0 mV) without significantly affecting expression with peak currents of 1.3 ± 0.4 μA ($n = 10$) for α_{1E} alone and 1.7 ± 0.5 μA ($n = 6$) for α_{1E}/β_{2a} channels. On the other hand, α_{1C}/β_{2a} channels displayed a 5-fold increase in peak macroscopic current expression as compared to α_{1C} channels, a negative shift in the peak current, but showed little change on macroscopic inactivation properties (Perez-Reyes et al., 1992; Parent et al., *unpublished observations*). These results confirm that β subunit-regulation of calcium channel activity is dependent upon the nature of the α_1 subunit.

As seen in Fig. 4 *A, B, C,* coexpression with either β_{2a} or $\alpha_{2b}\delta$ failed to significantly increase α_{1E} whole-cell currents (*see also* Table 1). Nevertheless, coexpression with both β_{2a} and $\alpha_{2b}\delta$ subunits resulted in a 9 ± 2 ($n = 6$) -fold increase of whole-cell Ba^{2+} currents from 1.3 ± 0.4 μA ($n = 10$) for α_{1E} to 15 ± 5 μA ($n = 6$) for $\alpha_{1E}/\alpha_{2b}\delta/\beta_{2a}$ (Fig. 4*D*), suggesting a synergistic coupling between auxiliary subunits in α_{1E} channels. The accrued current expression with both auxiliary subunits is similar to what has been reported for $\alpha_{1A}/\alpha_{2b}\delta/\beta_{1b}$ *vs.* $\alpha_{1A}/\alpha_{2b}\delta$ and α_{1A}/β_{1b} (DeWaard & Campbell, 1995). In addition, the macroscopic *I-V* curve for $\alpha_{1E}/\alpha_{2b}\delta/\beta_{2a}$ peaked at 0 ± 2 mV ($n = 10$) indicating that the +10 mV positive shift caused by $\alpha_{2b}\delta$ and the −10 mV negative shift caused by β_{2a} have canceled each other out in $\alpha_{1E}/\alpha_{2b}\delta/\beta_{2a}$. Despite their differences in macroscopic peak currents, $\alpha_{1E}/\alpha_{2b}\delta/\beta_{2a}$ and α_{1E}/β_{2a} channels displayed identical activation and inactivation kinetics, suggesting that the neuronal $\alpha_{2b}\delta$ subunit does not reverse the effect of β subunits on α_{1E} kinetics, unlike previously reported for the skeletal $\alpha_{2b}\delta$ subunit (Wakamori et al., 1994). α_{1E}/β_{2a} and $\alpha_{1E}/\alpha_{2b}\delta/\beta_{2a}$ channel inactivation kinetics are virtually identical. The results obtained with α_{1E} channels contrast with the reported effects of the neuronal $\alpha_{2b}\delta$ and the skeletal $\alpha_{2b}\delta$ on the activation and inactivation kinetics of α_{1C} calcium channels (Singer et al., 1991; Hullin et al., 1992; L. Parent et al., *unpublished observations*).

These changes in α_{1E} channel kinetics were correlated to similar changes in the steady-state properties of channel inactivation. The voltage-dependence of inactivation for α_{1E} channels was investigated in the presence of the same channel composition. Figure 5 shows whole-cell current traces obtained in the presence of 10

Table 2. β-induced peak current stimulation of α_{1E} channels

Subunit composition	Mean peak current ± SEM	*n*	Batch
$\alpha_{1E}/\alpha_{2b}\delta/\beta_{1a}$	−2.9 ± 0.5 μA	5	X852
$\alpha_{1E}/\alpha_{2b}\delta/\beta_{1b}$	−1.8 ± 0.2 μA	6	X852
$\alpha_{1E}/\alpha_{2b}\delta/\beta_{2a}$	−3.0 ± 0.4 μA	6	X852
$\alpha_{1E}/\alpha_{2b}\delta/\beta_{3}$	−0.7 ± 0.1 μA	5	X852
$\alpha_{1E}/\alpha_{2b}\delta/\beta_{4}$	−0.8 ± 0.1 μA	6	X852

Comparison of the peak current amplitudes obtained for different $\alpha_{1E}/\alpha_{2b}\delta/\beta_x$ channel compositions. Since mRNA translational efficiency was found to vary between batches, all data reported here were collected within the same oocyte batch. The number *n* of experiments for each channel is indicated. Data are mean ± SEM. Currents were measured with 10 mM Ba^{2+} as the charge carrier. Holding potential was −80 mV.

mM Ba^{2+}, for α_{1E}; $\alpha_{1E}/\alpha_{2b}\delta$; α_{1E}/β_{2a}; and $\alpha_{1E}/\alpha_{2b}\delta/\beta_{2a}$ channels (Fig. 5 *A–D*). Steady-state inactivation was measured after a series of 5-sec prepulses applied between −80 to +20 mV from a holding potential of −100 mV. Normalized current amplitudes were compiled for $n = 4$, plotted against the prepulse voltage, and mean data points were fitted to a modified Boltzmann equation (Eq. 1). Fits to the mean inactivation data points are shown. As seen, α_{1E} and $\alpha_{1E}/\alpha_{2b}\delta$ currents inactivated completely within the 5-sec prepulse with midpoint of inactivation $E_{0.5} = -50$ mV for α_{1E} and $E_{0.5} = -44$ mV for $\alpha_{1E}/\alpha_{2b}\delta$ channels. The rightward shift observed for $\alpha_{1E}/\alpha_{2b}\delta$ channels might be related to the +10 mV shift of their peak current *I-V* curve. Coexpression with β_{2a} subunit shifted further the midpoint of inactivation $E_{0.5}$ to the right from −50 mV (α_{1E}) to −31 mV (α_{1E}/β_{2a}) with a substantial fraction (45%) of noninactivating Ba^{2+} current. Inactivation data points were identical for α_{1E}/β_{2a} and $\alpha_{1E}/\alpha_{2b}\delta/\beta_{2a}$ channels confirming that $\alpha_{2b}\delta$ has little additional effect on α_{1E}/β_{2a} channel inactivation, that is β_{2a} appeared to have a dominant effect on α_{1E} inactivation.

β Subunit Regulation of the Human Brain α_{1E}

To determine whether other cloned brain Ca^{2+} channel subunits may functionally interact with α_{1E} channels, we performed a series of coexpression studies with rat brain β_{1b}, β_{2a}, β_3, and β_4 subunits. All subunit channel composition were injected in the same oocyte population and studied within 5 days after injection. Coexpression with any β subunit increased the average size of the Ba^{2+} current recorded as compared to α_{1E} and $\alpha_{1E}/\alpha_{2b}\delta$ currents measured the same day. Table 2 shows the average peak current measured for each channel composition. Figure 6 shows macroscopic current traces recorded after injection in *Xenopus* oocytes of mRNA coding for $\alpha_{1E}/\alpha_{2b}\delta/\beta_3$; $\alpha_{1E}/\alpha_{2b}\delta/\beta_{1b}$; $\alpha_{1E}/\alpha_{2b}\delta/\beta_{1a}$; $\alpha_{1E}/\alpha_{2b}\delta/\beta_4$; and $\alpha_{1E}/\alpha_{2b}\delta/\beta_{2a}$. The calcium channel $\alpha_{1E}/\alpha_{2b}\delta/\beta_{2a}$ is the only channel combination that produced whole-cell Ba^{2+} currents with slower inactivation than α_{1E} channels. As shown in Table 3, all channels activated with a single time constant τ_{act} ranging from 3 to 3.6 msec. Macroscopic currents generally peaked between 4 and 7 msec after the pulse. For all α_{1E} channels but for $\alpha_{1E}/\alpha_{2b}\delta/\beta_{2a}$, Ba^{2+} currents were best described by a sum of two time constants with the most important being the fast τ^1_{inact} in the 10 to 20 msec range and a minor contribution from the slower τ^2_{inact} in the 100 to 160 msec range. Coinjection with β_{1b} generated whole-cell currents with inactivation kinetics faster than with β_{1a}. Mean normalized *I-V* curves show that whole-cell currents activated sensibly around −40 mV in the presence of 10 mM Ba^{2+} with no appreciable difference between channel composition as shown from data obtained from 5 independent experiments. Whole-cell currents peaked at −10 mV for $\alpha_{1E}/\alpha_{2b}\delta/\beta_{1b}$; $\alpha_{1E}/\alpha_{2b}\delta/\beta_{1a}$ and $\alpha_{1E}/\alpha_{2b}\delta/\beta_{2a}$ channels

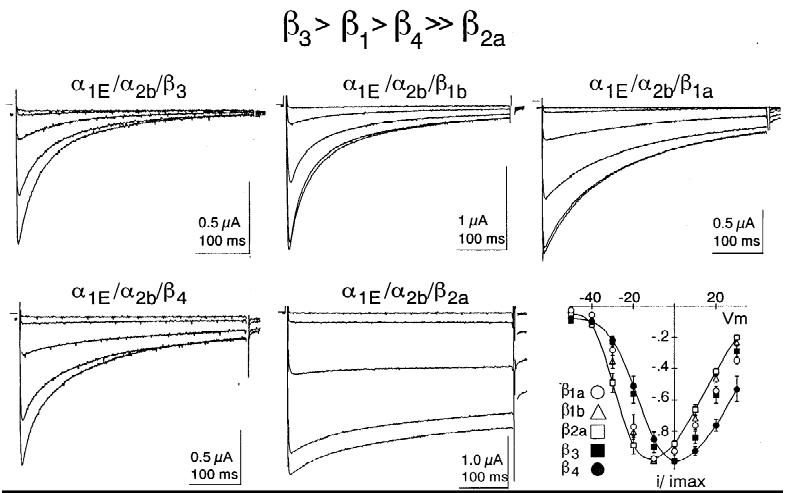

Fig. 6. β subunit modulation of α_{1E} whole-cell currents measured in the presence of 10 mM Ba^{2+}. The neuronal $\alpha_{2b}\delta$ subunit was present throughout. Holding potential = −80 mV. Current traces shown were recorded from the same frog donor. Current traces were fitted to a sum of three (3) exponential functions; τ_{act}; τ^1_{inact}; τ^2_{inact}. For a pulse from −80 to −10 mV, the time constants were the following (τ_{act}; τ^1_{inact}; τ^2_{inact}); $\alpha_{1E}/\alpha_{2b}\delta/\beta_3$ (3 msec; 18 msec; 107 msec); $\alpha_{1E}/\alpha_{2b}\delta/\beta_{1b}$ (3 msec; 23 msec; 126 msec); $\alpha_{1E}/\alpha_{2b}\delta/\beta_{1a}$ (3 msec; 19 msec; 172 msec); $\alpha_{1E}/\alpha_{2b}\delta/\beta_4$ (3 msec; 20 msec; 181 msec). Only two time constants, $\tau_{act} = 3$ msec and $\tau_{inact} = 173$ msec, were required to fit the $\alpha_{1E}/\alpha_{2b}\delta/\beta_{2a}$ current traces.

Table 3. $\alpha_{1E}/\alpha_{2b}\delta/\beta_x$ whole-cell current time constants

Subunit composition	τ activation (msec)	τ^1 inact (msec)	τ^2 inact (msec)	*n*
$\alpha_{1E}/\alpha_{2b}\delta/\beta_{1a}$	3.0 ± 0.1	20 ± 5	145 ± 20	5
$\alpha_{1E}/\alpha_{2b}\delta/\beta_{1b}$	3.6 ± 0.3	17 ± 3	120 ± 18	6
$\alpha_{1E}/\alpha_{2b}\delta/\beta_{2a}$	3.0 ± 0.1		235 ± 31	11
$\alpha_{1E}/\alpha_{2b}\delta/\beta_3$	3.5 ± 0.2	16 ± 4	109 ± 13	5
$\alpha_{1E}/\alpha_{2b}\delta/\beta_4$	2.9 ± 0.4	20 ± 5	158 ± 15	6

Activation and inactivation time constants measured at −10 mV, from $\alpha_{1E}/\alpha_{2b}\delta$ channels coinjected with different β subunits. Current traces were fitted to Eq. 2. The time course of inactivation was best fitted by a sum of 2 exponential functions but for $\alpha_{1E}/\alpha_{2b}\delta/\beta_{2a}$ channels. Each time constant is the mean of 5 to 11 experiments measured with 10 mM Ba^{2+} as the charge carrier. Holding potential was −80 mV.

and at 0 mV for $\alpha_{1E}/\alpha_{2b}\delta/\beta_4$ and $\alpha_{1E}/\alpha_{2b}\delta/\beta_3$ channels. β-induced rates of inactivation were (from fastest to slowest) $\beta_3 > \beta_1 > \beta_4 \gg \beta_2$. The potency order was similar to the one found for α_{1C} (Hullin et al., 1992) and α_{1A} (Sather et al., 1993) who found $\beta_3 > \beta_1 > \beta_2$ in their respective channels. Since the α_{1C} recombinant channel has been the most widely studied calcium channel, it remains the standard for β-subunit induced regulation. To compare our β-subunit regulation data on α_{1E} to published data, we performed a similar series of experiments on the recombinant α_{1C} channel. Figure 7 shows whole-cell current traces recorded in the presence of 120 mM Li^+ (left), 10 mM Ba^{2+} (middle), and 10 mM Ca^{2+} (right) for the rabbit cardiac calcium channel $\alpha_{1C}/\alpha_{2b}/\beta_{1a}$ (first row), $\alpha_{1C}/\alpha_{2b}/\beta_{2a}$ (second row), $\alpha_{1C}/\alpha_{2b}/\beta_3$ (third row), and $\alpha_{1C}/\alpha_{2b}/\beta_4$ (last row). The whole-cell α_{1C} currents were typically faster when measured in the presence of Ca^{2+} for it is known that this channel exhibits calcium-dependent inactivation. Nonetheless, as for the α_{1E} calcium channel, β_{1a} and β_3 induced faster inactivating currents than β_{2a} and β_4. This observation holds true whether currents were measured in Li^+, Ba^{2+} or Ca^{2+}. Steady-state inactivation data were collected in the presence of 10 mM Ba^{2+} using the same pulse protocol. Figure 8 compares the β-induced modulation of steady-state inactivation properties for α_{1C} and α_{1E} calcium channels in the presence of the neuronal $\alpha_{2b}\delta$ subunit. Inactivation was measured after a 5-sec prepulse to −10 mV from a holding potential of −60 mV (α_{1C}) or −80 mV (α_{1E}). Each set of experiments was repeated 4 to 6 times. As seen, coexpression with β_3 or β_{1b} resulted in more complete inactivation than coexpression with β_{2a} for both α_{1C} and α_{1E} channels. In addition, the voltage-dependence of inactivation was systematically more negative for β_3 or β_{1b}-coexpressing channels. The main difference turned out in β_4-induced channel modulation. In our experiments, coinjection with β_4 produced fast and complete inactivation of α_{1E} channels shifting the midpoint of inactivation from −54 mV for α_{1E} to −60 mV for

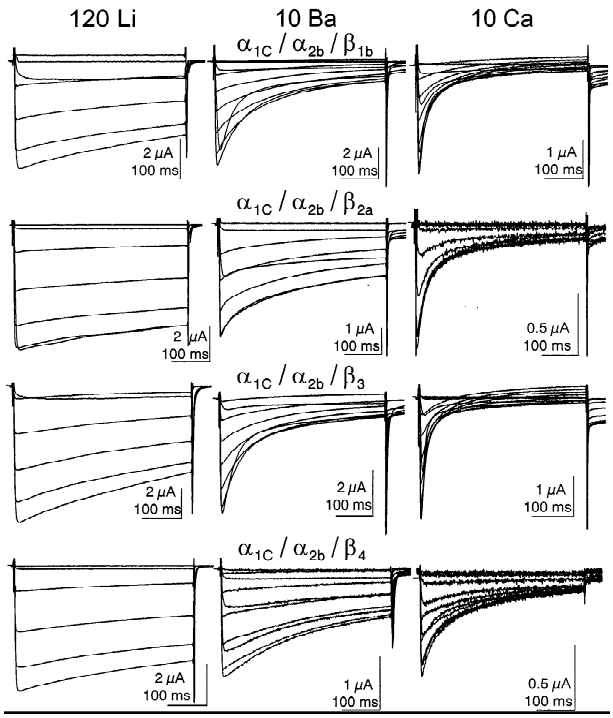

Fig. 7. Whole-cell current traces recorded for the rabbit cardiac α_{1C} in the presence of 120 mM Li^+ (left); 10 mM Ba^{2+} (middle); and 10 mM Ca^{2+} (right) after injection of 10 mM Bapta. Holding potential was −60 mV throughout. 450 msec voltage pulses were applied from −60 to +30 mV. The a1C channel was co-injected with $\alpha_{2b}\delta$ throughout, and β_{1a} (top row); β_{2a} (second row); β_3 (third row); and β_4 (last row). Capacitive transients were erased for the first msec after the voltage step. Current scales vary between 0.5 and 2 μA and time scales are 100 msec throughout.

$\alpha_{1E}/\alpha_{2b}\delta/\beta_4$ channels. However, despite producing a significant 5-fold increase of α_{1C} peak currents, β_4 had surprisingly very little effect on α_{1C} channel inactivation time constants and voltage-dependence. This lack of effect on α_{1C} inactivation kinetics was unexpected considering since β_4 has been previously reported to speed up inactivation kinetics of rabbit α_{1C} calcium channels (Castellano et al., 1993*b*). Overall, β-induced regulation can be said to occur in the following order (from fastest to slowest) for both α_{1C} and α_{1E}: $\beta_3 > \beta_1 \gg \beta_2$.

Discussion

In the present study, we have examined the functional properties of recombinant α_{1E} calcium channels in the presence, and in the absence of auxiliary subunits. The high level of α_{1E} calcium channel expression in the absence of auxiliary subunits, has made this subunit an appropriate model to study subunit-subunit interaction in calcium channels. This feature was especially critical to rule out kinetic contamination from endogenous calcium

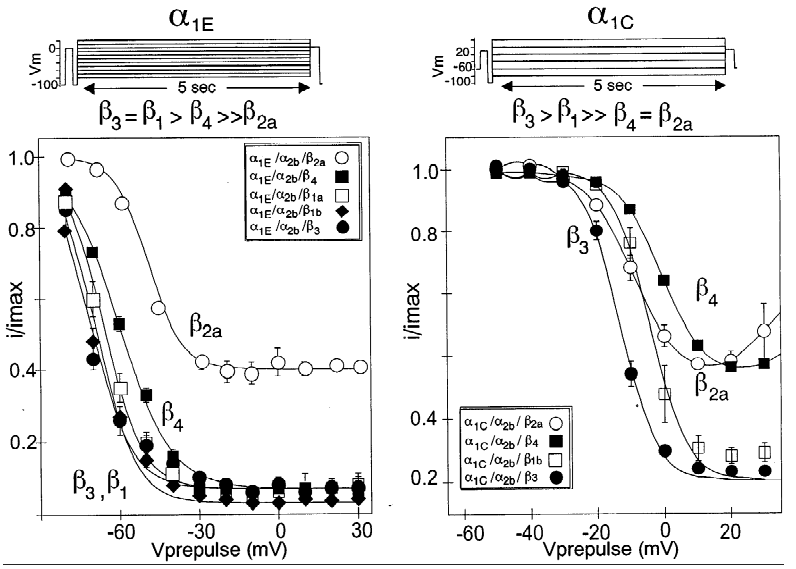

Fig. 8. Comparison of steady-state inactivation curves obtained for α_{1E} (left) and α_{1C} (right). Steady-state inactivation curves were measured in the presence of 10 mM Ba^{2+} after a series of 5-sec prepulse applied from −80 to +30 mV. *Left panel.* α_{1E} current traces obtained with β_{1a}; β_{1b}; β_3; β_4 inactivated completely after a 5-sec prepulse while only 60% of the $\alpha_{1E}/\alpha_{2b}\delta/\beta_{2a}$ current inactivated after a pulse to +30 mV. Coinjection with β_{1a}; β_{1b}; β_3 and β_4 induced a leftward shift in the midpoint of inactivation $E_{0.5}$ from −54 mV; (α_{1E} alone) to; −60 mV ($\alpha_{1E}/\alpha_{2b}\delta/\beta_4$); −66 mV ($\alpha_{1E}/\alpha_{2b}\delta/\beta_{1a}$); −69 mV ($\alpha_{1E}/\alpha_{2b}\delta/\beta_{1b}$); −73 mV ($\alpha_{1E}/\alpha_{2b}\delta/\beta_3$). Only coinjection with β_{2a} induced a shift to the right with a midpoint of inactivation $E_{0.5}$ = −42 mV. Slope steepness or *z* factor were 2.9 ($\alpha_{1E}/\alpha_{2b}\delta/\beta_4$); 3.4 ($\alpha_{1E}/\alpha_{2b}\delta/\beta_{1a}$); 3.4 ($\alpha_{1E}/\alpha_{2b}\delta/\beta_{1b}$); 3.3 ($\alpha_{1E}/\alpha_{2b}\delta/\beta_3$); 3.4 ($\alpha_{1E}/\alpha_{2b}\delta/\beta_{2a}$). *Right panel.* Experimental conditions were identical but for the holding potential that was −60 mV for α_{1C} and −80 mV for α_{1E} channels. For $\alpha_{1C}/\alpha_{2b}\delta/\beta_3$ and $\alpha_{1C}/\alpha_{2b}\delta/\beta_{1b}$, current traces inactivated completely after a 5-sec prepulse to 0 mV while only 60% of the $\alpha_{1C}/\alpha_{2b}\delta/\beta_4$ and $\alpha_{1C}/\alpha_{2b}\delta/\beta_{2a}$ currents inactivated completely. Coinjection with β_{1b}; β_{2a}; and β_3 induced a leftward shift in the midpoint of inactivation from −10 mV for α_{1C} alone; to −16 mV for $\alpha_{1C}/\alpha_{2b}\delta/\beta_{2a}$; to −24 mV for $\alpha_{1C}/\alpha_{2b}\delta/\beta_{1b}$; to −34 mV for $\alpha_{1C}/\alpha_{2b}\delta/\beta_3$. Steady-state inactivation of $\alpha_{1C}/\alpha_{2b}\delta/\beta_4$ currents occurred at voltage more positive with $E_{0.5}$ = −3 mV. Slope steepness or *z* factor; varied from 2.9 ($\alpha_{1C}/\alpha_{2b}\delta/\beta_4$); 3.4 ($\alpha_{1C}/\alpha_{2b}\delta/\beta_{1a}$); 3.4 ($\alpha_{1C}/\alpha_{2b}\delta/\beta_{1b}$); 3.3 ($\alpha_{1C}/\alpha_{2b}\delta/\beta_3$); 3.4 ($\alpha_{1C}/\alpha_{2b}\delta/\beta_{2a}$).

channels in *Xenopus* oocytes which is more likely to be observed in the presence of auxiliary subunits (Lacerda et al., 1994). Expression of the human α_{1E} subunit alone yielded fast inactivating currents. Coexpression with the human neuronal $\alpha_{2b}\delta$ subunit shifted the peak current from 0 to +10 mV without increasing peak current expression or modulating inactivation rate constants. Coexpression with β subunits modulated whole-cell kinetics with β_{2a} significantly slowing down α_{1E} inactivation.

Regulation of α_{1E} Inactivation by the Charge Carrier

The human α_{1E} channel studied in this work is a splice variant of the α_{1E} channel that has been previously functionally cloned and characterized from different species such as rat (Soong et al., 1993); rabbit (Wakamori et al., 1994); human (Schneider et al., 1994; Williams et al., 1994); and marine ray *doe*-1 (Ellinor et al., 1993). It is generally agreed that functional expression of α_{1E} channels produces fast inactivating Ba^{2+} currents whether α_{1E} is expressed in *Xenopus* oocytes (Soong et al., 1993; Wakamori et al., 1994; Schneider et al., 1994; Ellinor et al., 1993) or in mammalian cells (Williams et al., 1994). As suggested by the *I-V* curves in Figs. 1 and 6, under physiological conditions in the presence of 1.8 mM Ca^{2+}, α_{1E} channels would probably activate between −50 mV (Li^+, no Ca^{2+}) and −40 mV (10 mM Ca^{2+}). Thus, α_{1E} channels would activate at voltages more positive than −70 mV where low-voltage-activated calcium channels classically activate (Hille, 1992).

As observed previously, Ba^{2+} currents showed fast inactivation kinetics in the absence of auxiliary subunits (Soong et al., 1993; Schneider et al., 1994; this study), a fact that was interpreted as to the lack of Ca-inactivation in this channel (DeLeon et al., 1995). Perhaps the most striking observation reported herein is that whole-cell currents generated after expression of the α_{1E} subunit alone, can display slightly faster inactivation kinetics in the presence of divalent cations (such as Ca^{2+} and Ba^{2+}) than in the presence of monovalent cations such as Li^+, with inactivation being faster for $Ca^{2+} \geqslant Ba^{2+} > Li^+$. Although the charge carrier contribution to α_{1E} inactivation turned out to be unquestionably less dramatic than for α_{1C} channels, it was nonetheless significant especially for α_{1E} alone. This suggests that the calcium-binding site may exist on α_{1E} with however a much lower affinity for Ca^{2+} than on α_{1C}. Recent structure-function studies identified potential sites on the C-terminus as the locus for calcium-dependent inactivation in α_{1C} channels (DeLeon et al., 1995; Zhou et al., 1997). As reported by others (DeLeon et al., 1995; Zhou et al., 1997), we however observed that Ca^{2+} and Ba^{2+} inactivation seems to occur with similar rates in α_{1E}/β_{2a} channels (*data not shown*). It would be highly interesting to compare the Ca^{2+} affinity produced by C-terminus-like peptides of both α_{1C} and α_{1E} channels and study a possible modulation role by the β subunit.

Regulation of α_{1E} Channels by the $\alpha_{2b}\delta$ Subunit

As observed for α_{1C} and α_{1A} calcium channels, α_{1E} activation and inactivation kinetics were found to be modu-

lated by β and $\alpha_2\delta$ subunits although there were subtle differences in the nature of the α_{1E} channel regulation. We found that coexpression with $\alpha_{2b}\delta$ alone had little effect on α_{1E} inactivation kinetics, and on α_{1E} current expression. These results are similar to results obtained on the α_{1A} calcium channel (DeWaard & Campbell, 1995). The only change brought about by the presence of $\alpha_{2b}\delta$, in our experiments, was a small but significant, positive shift in the voltage-dependence of α_{1E} activation as measured from peak current-voltage relationships, and a similar shift on the voltage-dependence of steady-state inactivation which were absent in the α_{1A} channel. This rightward shift in the peak current *I-V* thus suggests some functional interaction between the $\alpha_{2b}\delta$ and the α_{1E} subunit. Furthermore, additional coinjection with β_{2a} was shown to cancel out the effect of $\alpha_{2b}\delta$ on the α_{1E} current-voltage relationship such that $\alpha_{1E}/\alpha_{2b}\delta/\beta_{2a}$ and α_{1E} channels both peaked at 0 mV. To our knowledge, there is only one published report of a $\alpha_2\delta$ modulation on neuronal calcium channel macroscopic current kinetics. In rabbit brain α_{1E} channels (BII), coinjection of skeletal $\alpha_{2a}\delta$ to α_{1E}/β_1 channels produced whole-cell currents with similar inactivation than rabbit BII channels, which indicate that $\alpha_{2a}\delta$ seemingly canceled out the effect of the β_1 subunit (Wakamori et al., 1994). The discrepancy between the two studies might be explained by the intrinsic differences of the $\alpha_2\delta$ splice variant used, for the skeletal $\alpha_{2a}\delta$ alone is also known to modulate recombinant α_{1C} calcium currents (Singer et al., 1991). Thus, β subunit-induced shifts of macroscopic current kinetics were not affected by the presence of the $\alpha_{2b}\delta$ subunit in α_{1A} (DeWaard & Campbell, 1995) and in brain α_{1E} channels (this study). Hence, $\alpha_{1E}/\alpha_{2b}\delta/\beta_{2a}$ and α_{1E}/β_{2a} whole-cell currents displayed similar rate of macroscopic inactivation.

Our experiments showed that coexpression with both $\alpha_{2b}\delta$ and β subunits was required to maximally stimulate functional expression of the human brain α_{1E} channel with a ≈10-fold increase in expression levels. Expression with $\alpha_{2b}\delta$ was also shown to increase the β_1 and the β_4 subunit stimulation of α_{1A} whole-cell currents (DeWaard & Campbell, 1995; Gurnett et al., 1996). In other words, the role of $\alpha_{2b}\delta$ on whole-cell currents appeared to be more prominent in the presence of a β subunit suggesting a synergistic effect between the calcium channel subunits on protein expression.

Regulation of α_{1E} Channels by β Subunits

We analyzed the differences in current properties introduced by the presence of the four genes coding for β subunits and used these differences as an index of the functional contribution of each of these auxiliary subunits in α_{1E} function. Our findings demonstrate that β_{1a}; β_{1b}; β_{2a}; β_3; and β_4 subunits interact functionally with the α_{1E} subunit. The major effect of β-subunit induced changes was to modulate α_{1E} activation and inactivation kinetics. Our expression data thus nicely mirrored recent reports that antisense depletion of β subunits decreased whole-cell calcium currents and shifted the voltage-dependence of current kinetics in neuronal cells (Berrow et al., 1995; Lambert et al., 1996).

The rate of inactivation generally increased after coexpression with β subunits with $\beta_3 > \beta_1 > \beta_4$ (from fastest to slowest) while β_{2a} actually slowed down α_{1E} inactivation kinetics. β subunit induced-hyperpolarizing shifts in the voltage-dependence of inactivation were also observed with these faster inactivation kinetics with $\beta_3 > \beta_1 > \beta_4 \gg \beta_{2a}$. Of all the subunit investigated in this study, β_{2a} subunit had the most dramatic effect by slowing down α_{1E} whole-cell currents whether currents were measured with Li^+ (*see* Fig. 3) or Ba^{2+} as the charge carrier. In the presence of 10 mM Ba^{2+}, about 45% of α_{1E}/β_{2a} channels remained in the activated state at the end of a 5-sec prepulse as opposed to <1% of α_{1E} channels. This observation has also been previously reported for the human α_{1E} (Olcese et al., 1994) and after coinjection of β_{2a} with α_{1A} (Stea et al., 1994; DeWaard & Campbell, 1995). In the latter, 60% of the Ba^{2+} whole-cell current remained for α_{1A}/β_{2a} channels as opposed to only 11% for α_{1A} channels when measured after a 2-sec prepulse. In α_{1C} calcium channels, β_{2a} caused faster activation kinetics, faster half-time to peak currents, and larger macroscopic currents (Perez-Reyes et al., 1992) but its effect on inactivation kinetics remained difficult to assess quantitatively, partly because α_{1C} alone expression is low, and partly because α_{1C} already displays slow inactivation kinetics. At best, one might conclude from the original whole-cell recordings (Perez-Reyes et al., 1992; Hullin et al., 1992) that there is no apparent change in the inactivation kinetics of α_{1C} after coinjection of β_{2a}. Despite these dramatic changes in α_{1E} kinetics, coexpression with β_{2a} did not modify the channel high affinity for Ca^{2+}. This result further confirms the absence of modulation of the β subunit on the calcium channel high affinity binding sites formed by the E residues in the pore region (Yang et al., 1993; Parent & Gopalakrishnan, 1995).

According to Neely and collaborators (1993), gating charge movement indicated that β_{2a} improved the intramolecular coupling between the voltage sensor and the channel pore opening in α_{1C}. In other words, coinjection with β_{2a} would speed up the closed-to-open transitions in α_{1C} which should translate into shorter latencies at the single channel level. In our experiments, α_{1E} and α_{1E}/β_{2a} channels activated with the same activation time constant, and displayed similar half-time to peak currents. Thus, our whole-cell data do not support a role for β_{2a} on the rate of the closed-to-open transitions in α_{1E} channels. Our data however indicated that β_{2a} proceeded to keep

the channel into the open state for a longer period of time than any other auxiliary subunit tested in this work. The slower macroscopic inactivation could result from either an increased open- to- closed state transition (shorter mean open time, more frequent reopenings); or from slower open- to- inactivated state transition (same mean open time, more frequent reopenings). Additionally, the situation might be even more complex and α_{1E} channels inactivation could occur through 2 distinct inactivated states (as suggested by its 2 time constants τ^1_{inact} and τ^2_{inact}). In this last kinetic scheme, the addition of the β_{2a} subunit could be disrupting the equilibrium between these two inactivated states such that the ''slower'' inactivated state appears to be dominant. The possible kinetic models are endless and evidently, our whole-cell data do not allow us to discriminate between models. Such information can only be extracted from single-channel recordings which are beyond the scope of this paper.

The apparent similarity of the overall gating mechanism between voltage-dependent channels suggests that molecular mechanisms can also be related. Given the physical proximity of IS6, the putative locus of voltage-dependent inactivation in calcium channels (Zhang et al., 1994), and the I-II linker, where β subunits are believed to bind (Pragnell et al., 1994), one can imagine that β-induced changes in inactivation can be caused by some interaction between the β subunit and IS6. In this scheme, β_{2a} could potentially interfere with the inactivation mechanism of α_{1E} through some interaction with its inactivation locus. This model could even be compatible with a ball-and-chain mechanism whereby β subunits, in general, could modulate the interaction between the inactivation ball (which remains unidentified) and its receptor in IS6 (Zhang et al., 1994).

As reported for α_{1C} and α_{1A} channels, coinjection with β_3 and β_1 subunits generate α_{1E} calcium channels with apparent faster inactivation kinetics (Hullin et al., 1992; Castellano et al., 1993*a;* Sather et al., 1993; Stea et al., 1994; DeWaard & Campbell, 1995). Coexpression with β1 subunits was also shown to generate faster inactivation kinetics on the rat brain α_{1E} channel (Soong et al., 1993) and the human α_{1E} channel (Olcese et al., 1994). Only the rabbit brain α_{1E} calcium channel appeared to display slower kinetics after coinjection with the brain β1 subunit (Wakamori et al., 1994). The effect of the β_4 subunit on channel kinetics turned out to be more channel-dependent. In neuronal channels, such as for α_{1A} (Stea et al., 1994; DeWaard & Campbell, 1995) and α_{1E} (our study), coinjection with β_4 appeared to produce little effect on channel inactivation kinetics despite producing clear negative shifts in the *I-V* relations and voltage-dependence of inactivation. These results sharply contrast with similar experiments performed with full-length α_{1C} channels where it was shown that β_4 produced faster inactivation kinetics without affecting the voltage-dependence of inactivation (Castellano et al., 1993*b*). However, unlike the original report, our α_{1E} study was performed in the continual presence of the neuronal $\alpha_{2b}\delta$ which could have affected whole-cell current kinetics. This discrepancy thus prompted us to characterize the β-induced voltage-dependence of inactivation of α_{1C} channels in the presence of the $\alpha_{2b}\delta$ subunit. Interestingly, our results with $\alpha_{1C}/\alpha_{2b}\delta/\beta_4$ channels confirmed the previous observation made by Castellano et al., (1993*b*) that coinjection with β_4 does not shift the voltage-dependence of α_{1C} inactivation. However, $\alpha_{1C}/\alpha_{2b}\delta/\beta_4$ channels displayed slower inactivation kinetics than previously reported for α_{1C}/β_4 channels (Castellano et al., 1993*b*). In fact, according to the reports published by this group, β_4 would induce faster inactivation kinetics than β_3 (Castellano et al., 1993*a,b*). There is still a slight possibility that $\alpha_{2b}\delta$ makes a difference although $\alpha_{2b}\delta$ has never been reported to slow down inactivation kinetics. The possibility that the differences between the 2 studies might be explained by low β_4 mRNA translational efficiency was also ruled out since our whole-cell $\alpha_{1C}/\alpha_{2b}\delta/\beta_4$ currents averaged 2.2 ± 0.3 μA (*see* Fig. 7). It remains however to be seen whether the kinetics differences can be due to the presence of the deleted version of the α_{1C} (α_{1C} ΔNΔC) channel, although this version has been shown before to behave mostly like the full-length channel.

In summary, our results illustrated the wide variety of biophysical properties that can be generated by a single calcium channel α_1 subunit, depending on the associating β subunit. This observation was especially apt in the case of the α_{1E} and the β_{2a} subunits. Expression of the α_{1E} channel gave rise to fast inactivating channels while coexpression with β_{2a} subunit yielded channels with slower kinetics. The combination of expression and structural data are thus needed to elucidate the nature of calcium channels present in neuronal cells.

We thank Dr. Terry P. Snutch for the rat brain $\alpha_{2b}\delta$ subunit; Dr. Ed Perez-Reyes for the β_{1b}, β_{2a}, β_3, and β_4 subunits; Dr. F. Hofmann for the β_{1a} subunit; T. Rodriguez, D. Medrano, G. Bernatchez for technical assistance; and colleagues from the Membrane Transport Research Group for comments and discussion. L.P. is a *Junior 2* scholar from the Fonds de la Recherche en Santé du Québec. This work was funded through grants from the National Institutes of Health HL54708; the Canadian Heart and Stroke Foundation; and the Medical Research Council of Canada to L.P.

References

Berrow, N.S., Campbell, V., Fitzgerald, E.M., Brickley, K., Dolphin, A.C. 1995. Antisense depletion of β-subunits modulates the biophysical and pharmacological properties of neuronal calcium channels. *J. Physiol.* **482:**481–491

Brickley, K., Campbell, V., Berrow, N., Leach, R., Norman, R.I., Wray, D., Dolphin, A.C., Baldwin, S.A. 1995. Use of site-directed

antibodies to probe the topography of the α_2 subunits of voltage-gated Ca^{2+} channels. *FEBS Lett.* **364:**129–133

Brust, P.F., Simerson, S., McCue, A.F., Deal, C.R., Schoonmaker, S., Williams, M.E., Veliçelebi, G., Johnson, E.C., Harpold, M.M., Ellis, S.B. 1993. Human neuronal voltage-dependent calcium channels: studies on subunit structure and role in channel assembly. *Neuropharm.* **32:**1089–1102

Castellano, A., Wei, X., Birnbaumer, L., Perez-Reyes, E. 1993*a*. Cloning and expression of a third calcium channel β subunit. *J. Biol. Chem.* **268:**3450–3455

Castellano, A., Wei, X., Birnbaumer, L., Perez-Reyes, E. 1993*b*. Cloning and expression of a neuronal calcium channel β subunit. *J. Biol. Chem.* **268:**12359–12366

Catterall, W.A. 1991. Functional subunit structure of voltage-gated calcium channels. *Science* **250:**1499–1500

DeLeon, M., Wang, Y., Jones, L., Perez-Reyes, E., Wei, X., Soong, T.W., Snutch, T.P., Yue, D.T. 1995. Essential Ca^{2+}-binding motif for Ca^{2+}-sensitive inactivation of L-type Ca^{2+} channels. *Science* **270:**1502–1506

DeWaard, M., Campbell, K.P. 1995. Subunit regulation of the neuronal α_{1A} Ca^{2+} channel expressed in *Xenopus* oocytes. *J. Physiol.* **485:**619–634

Ellinor, P., Zhang, J-F., Randall, A.D., Zhou, M., Schwarz, T.L., Tsien, R.W., Horne, W.A. 1993. Functional expression of a rapidly inactivating neuronal calcium channel. *Nature* **363:**455–458

Ellis, S.B., Williams, M.E., Ways, N.R., Brenner, R., Sharp, A.H., Leung, A.T., Campbell, K.P., McKenna, E., Koch, W.J., Hui, A., Schwartz, A., Harpold, M.M. 1988. Sequence and expression of mRNAs encoding the α_1 and α_2 subunits of a DHP-sensitive calcium channel. *Science* **241:**1661–1664

Fabiato, A., Fabiato, F. 1979. Calculator programs for computing the composition of the solutions containing multiple metals and ligands used for experiments in skinned muscle cells. *J. Physiol.* **75:**463–505

Gurnett, C.A., DeWaard, M., Campbell, K.P. 1996. Dual function of the voltage-dependent Ca^{2+} channel $\alpha_2\delta$ subunit in current stimulation and subunit interaction. *Neuron* **16:**431–440

Hille, B. 1992. Ionic Channels of Excitable Membranes. Sinauer, Sunderland MA

Hullin, R., Singer-Lahat, D., Freichel, M., Biel, M., Dascal, N., Hofmann, F., Flockerzi, V. 1992. Calcium channel β subunit heterogeneity: functional expression of cloned cDNA from heart, aorta and brain. *EMBO J.* **11:**885–890

Lacerda, A.E., Kim, H.S., Ruth, P., Perez-Reyes, E., Flockerzi, V., Hofmann, F., Birnbaumer, L., Brown, A.M. 1991. Normalization of current kinetics by interaction between the α_1 and β subunits of the skeletal muscle dihydropyridine-sensitive Ca^{2+} channel. *Nature* **352:**527–530

Lacerda, A.E., Perez-Reyes, E., Wei, X., Castellano, A., Birnbaumer, L., Brown, A.M. 1994. T-type and N-type calcium channels of *Xenopus* oocytes: Evidence for specific interactions with β subunits. *Biophys. J.* **66:**1833–1843

Lambert, R.C., Maulet, Y., Dupont, J.L., Mykita, S., Carig, P., Volsen, S., Feltz, A. 1996. Polyethylenimine-mediated DNA transfection of peripheral and central neurons in primary culture: probing Ca^{2+} channel structure and function with antisense oligonucleotides. *Mol. Cell Neurosci.* **7:**239–246

Lory, P., Varadi, G., Slish, D.F., Varadi, M., Schwartz, A. 1993. Characterization of β subunit modulation of a rabbit cardiac L-type Ca^{2+} channel α_1 subunit as expressed in mouse L cells. *FEBS Lett.* **315:**167–175

Mori, Y., Friedrich, T., Kim, M.-S., Mikami, A., Nakai, J., Ruth, P., Bosse, E., Hofmann, F., Flockerzi, V., Furuichi, T., Mikoshiba, K., Tanabe, T., Numa, S. 1991. Primary structure and functional expression from complementary DNA of a brain calcium channel. *Nature* **350:**398–402

Neely, A., Wei, X., Olcese, R., Birnmbaumer, L., Stefani, E. 1993. Potentiation by the β subunit of the ratio of the ionic current to the charge movement in the cardiac calcium channel. *Science* **262:**575–578

Niidome, T., Kim, M.S., Friedrich, T., Mori, Y. 1992. Molecular cloning and characterization of a novel calcium channel from rabbit brain. *FEBS Lett.* **308:**7–13

Olcese, R., Qin, N., Schneider, T., Neely, A., Wei, X., Stefani, E., Birnbaumer, L. 1994. The amino acid terminus of a calcium channel β subunit sets rates of channel inactivation independently of the subunit's effect on activation. *Neuron* **13:**1433–1438

Parent, L., Gopalakrishnan, M. 1995*a*. Glutamate substitution in repeat IV alters monovalent and divalent permeation in the heart α_{1C} calcium channel. *Biophys. J.* **69:**1801–1813

Parent, L., Gopalakrishnan, M., Lacerda, A.E., Wei, X., Perez-Reyes, E. 1995*b*. Voltage-dependent inactivation in cardiac-skeletal chimeric calcium channels. *FEBS Lett.* **360:**144–150

Perez-Reyes, E., Castellano, A., Kim, H.S., Bertrand, P., Baggstrom, E., Lacerda, A.E., Wei, X., Birnbaumer, L. 1992. Cloning and expression of a cardiac/brain β subunit of the L-type calcium channel. *J. Biol. Chem.* **267:**1792–1797

Perez-Reyes, E., Wei, X., Castellano, A., Birnbaumer, L. 1990. Molecular diversity of L-type calcium channels. Evidence for alternative splicing of the transcripts of three non-allelic genes. *J. Biol. Chem.* **265:**20430–20436

Pragnell, M., DeWaard, M., Mori, Y., Tanabe, T., Snutch, T.P., Campbell, K.P. 1994. Calcium channel β subunit binds to a conserved motif in the I-II cytoplasmic linker of the α_1 subunit. *Science* **368:**67–70

Rodriguez, T., Schneider, T., Parent, L. 1996. Modulation of the human α_{1E} calcium channel by neuronal β and α_2 auxiliary subunits. *Biophys. J.* **70:**A184 (Abstr.)

Ruth, P., Röhrkasten, A., Biel, M., Bosse, E., Regulla, S., Meyer, H.E., Flockerzi, V., Hofmann, F. 1989. Primary structure of the β subunit of the DHP-sensitive calcium channel from skeletal muscle. *Science* **245:**1115–1118

Sambrook, J., Fritsch, E.F., Maniatis, T. 1989. Molecular Cloning: A Laboratory Manual. Cold Spring Harbor Laboratory, Cold Spring Harbor, New York

Sather, W.A., Tanabe, T., Zhang, J-F., Mori, Y., Adams, M.E., Tsien, R.W. 1993. Distinctive biophysical and pharmacological properties of class A (BI) calcium channel α_1 subunits. *Neuron* **11:**291–303

Schneider, T., Wei, X., Qin, N., Olcese, R., Costantin, J., Neely, A., Palade, P., Perez-Reyes, E., Qin, N., Zhou, J., Crawford, G.D., Smith, R.G., Appel, S.H., Stefani, E., Birnbaumer, L. 1994. Molecular analysis and functional expression of the human type E neuronal Ca^{2+}-channel α_1 subunit. *Receptors and Channels* **2:**255–270

Singer, D., Biel, M., Lotan, I., Flockerzi, V., Hofmann, F., Dascal, N. 1991. The roles of the subunits in the function of the calcium channel. *Science* **253:**1553–1557

Soong, T.W., Stea, A., Hodson, C.D., Dubel, S.J., Vincent, S.R., Snutch, T.P. 1993. Structure and functional expression of a member of the low voltage-activated calcium channel family. *Science* **260:**1133–1136

Stea, A., Dubel, S.J., Pragnell, M., Leonard, J.P., Campbell, K.P., Snutch, T.P. 1993. A β-subunit normalizes the electrophysiological properties of a cloned N-type Ca^{2+} channel α_1 subunit. *Neuropharm.* **32:**1103–1116

Stea, A., Tomlinson, W.J., Soong, T.W., Bourinet, E., Dubel, S.J., Vincent, S.R., Snutch, T.P. 1994. Localization and functional properties of a rat brain α_{1A} calcium channel reflect similarities to

neuronal Q- and P-type channels. *Proc. Natl. Acad. Sci. USA* **91:**10576–10580

Varadi, G., Lory, P., Schultz, D., Varadi, M., Schwartz, A. 1991. Acceleration of activation and inactivation by the β subunit of the skeletal muscle calcium channel. *Nature* **352:**159–162

Wakamori, M., Niidome, T., Furutama, D., Furuichi, T., Mikoshiba, K., Fujita, Y., Tanaka, I., Katayama, K., Yatani, A., Schwartz, A., Mori, Y. 1994. Distinctive functional properties of the neuronal BII (class E) calcium channel. *Receptors and Channels* **2:**303–314

Wei, X., Neely, A., Lacerda, A.E., Olcese, R., Stefani, E., Perez-Reyes, E., Birnbaumer, L. 1994*a*. Modification of Ca^{2+} channel activity by deletions at the carboxyl terminus of the cardiac α_1 subunit. *J. Biol. Chem.* **269:**1635–1640

Wei, X., Neely, A., Olcese, R., Stefani, E., Birnbaumer, L. 1994*b*. Gating and ionic current from N-terminal deletion mutants of the cardiac Ca^{2+} channel α_1 subunit. *Biophys. J.* **66:**A128 (*Abstr.*)

Wei, X., Pan, S., Lang, W., Kim, H., Schneider, T., Perez-Reyes, E., Birnbaumer, L. 1995. Molecular determinants of cardiac Ca^{2+} channel pharmacology. *J. Biol. Chem.* **270:**27106–27111

Wei, X., Perez-Reyes, E., Lacerda, A.E., Schuster, G., Brown, A.M., Birnbaumer, L. 1991. Heterologous regulation of the cardiac Ca^{2+} channel α_1 subunit by skeletal muscle β and ''gamma'' subunits. Implications for the structure of the cardiac L-type Ca^{2+} channels. *J. Biol. Chem.* **266:**21943–21947

Williams, M.E., Brust, P.F., Feldman, D.H., Patthi, S., Simerson, S., Maroufi, A., McCue, A.F., Velicilebi, G., Ellis, S.B., Harpold, M.M. 1992*b*. Structure and functional expression of an ω-conotoxin-sensitive human N-type calcium channel. *Science* **257:**389–395

Williams, M.E., Feldman, D.H., McCue, A.F., Brenner, R., Velicelebi, G., Ellis, S.B., Harpold, M.M. 1992*a*. Structure and functional expression of α_1, α_2, and β subunits of a novel human neuronal calcium channel subtype. *Neuron* **8:**71–84.

Williams, M.E., Marubio, L.M., Deal, C.R., Hans, M., Brust, P.F., Philipson, L.H., Miller, R.J., Johnson, E.C., Harpold, M.M., Ellis, S.B. 1994. Structure and functional characterization of neuronal α_{1E} calcium channel subtypes. *J. Biol. Chem.* **269:**22347–22357

Yang, J., Ellinor, P.T., Sather, W.A., Zhang, J.F., Tsien, R.W. 1993. Molecular determinants of Ca^{2+} selectivity and permeation in L-type Ca^{2+} channels. *Nature* **366:**158–161

Zhang, J.F., Ellinor, P.T., Aldrich, R.W., Tsien, R.W. 1994. Molecular determinants of voltage dependent inactivation in calcium channels. *Nature* **372:**97–100

Zhou, J. Olcese, R., Qin, N., Noceti, F., Birnbaumer, L., Stefani, E. 1997. Feedback inhibition of Ca^{2+} channels by Ca^{2+} depends on a short sequence of the C-terminus that does not include the Ca^{2+}-binding function of a motif with similarity to Ca^{2+}-binding domains. *Proc. Natl. Acad. Sci.* **94:**2301–2305